DOI: https://doi.org/10.24425/amm.2025.156255

W.H.B.M. SAUFEE®¹, L.W. KEONG®¹, A.S. SANGAR®¹, J.A WAHAB®¹,², N.I.M. NADZRI®¹,², VINH-DAT VUONG®³,⁴, A.A. MOHAMAD®⁵, A. ALSHOAIBI®⁶, M.F.M. NAZERI®¹,²\*

# GRAIN REFINEMENT AND HARDNESS IMPROVEMENT OF Sn-Zn SOLDERS WITH NICKEL-COATED PRECIPITATE CALCIUM CARBONATE

In this study, the effects of 0.5 wt.% of micro-sized and nano-sized nickel-coated precipitated calcium carbonate (PCC) on the structural, microstructural, and mechanical properties of tin-zinc (Sn-Zn) solder alloys were examined. X-ray diffraction analysis revealed the formation of a monoclinic  $Ni_3Sn_4$  phase, indicating significant structural transformation due to Ni-coating. Microstructural investigation showed refined Zn-rich grains in the composite solder alloys with micro-sized Ni-coated PCC, attributed to grain boundary strengthening. Elemental study confirmed a reduced Zn content of around 3.69 at.%, suggesting diffusion-induced redistribution during phase formation. Vickers microhardness testing using diamond indentation revealed that Sn-Zn added with micro-sized Ni-coated PCC exhibited the highest hardness at  $16.98 \pm 5$  HV, which is 12% higher than pure Sn-Zn solder. The results demonstrate the combined influence of phase reinforcement and microstructural evolution in enhancing the mechanical performance.

Keywords: Precipitate calcium carbonate; Composite solder; Grain refinement; Hardness; Surface modification

#### 1. Introduction

The eutectic tin-zinc (Sn-9Zn) alloy is a promising lead-free solder with a melting point of approximately 198°C, making it suitable for various electronic applications. Its single melting temperature at the eutectic composition also offers processing advantages during solidification [1]. However, the presence of Zn in this alloy often results in low corrosion resistance and poor wettability, limiting its performance [2]. To address these challenges, composite solders incorporating non-metal fillers have been introduced. Ceramic particles such as alumina [3], zinc oxide [4], and kaolin [5] have been employed to enhance various characteristics. For example in term of mechanical strength, it was reported that the additions of copper oxide significantly improved shear force of tin-silver-copper (SnAgCu) solder by 10.5 to 14.5% [6]. However, the corrosion exposure reduces the mechanical performance up to 24%, compared with the pristine SnAgCu. Similar trend was also seen for the zirconiaadded SnAgCu composite solder system [7]. While for thermal performance [8], increased void formation is seen with additions of silicon carbide in the matrix of SnAgCu-based solder leading to inferior properties.

Recently, precipitated calcium carbonate (PCC) has gained attention as a cost-effective and readily available filler material for composite solders [9]. Despite its advantages, ceramic fillers, including PCC, are prone to agglomeration due to density differences between the filler and solder matrix. This agglomeration leads to poor dispersion and uneven filler distribution, ultimately weakening interfacial bonding and mechanical properties [10]. Strategies such as ball milling [11], high-energy mixing [12], and the use of dispersants [13] or surfactants [14] have been explored to improve filler dispersion. Additionally, metal coatings on ceramic fillers, such as nickel (Ni), have shown potential in reducing agglomeration and enhancing compatibility with the solder matrix [10]. Nickel coatings are widely used for their durability, oxidation resistance, and ability to improve interfacial bonding

Corresponding author: firdausnazeri@unimap.edu.my



<sup>1</sup> UNIVERSITY MALAYSIA PERLIS (UNIMAP), FACULTY OF CHEMICAL ENGINEERING AND TECHNOLOGY, KOMPLEKS PUSAT PENGAJIAN JEJAWI 2, TAMAN MUHIBBAH, 02600 JEJAWI, ARAU, PERLIS, MALAYSIA

UNIVERSITI MALAYSIA PERLIS (UNIMAP), SURFACE TECHNOLOGY SPECIAL INTEREST GROUP, FACULTY OF CHEMICAL ENGINEERING AND TECHNOLOGY, 02600, ARAU, PERLIS, MALAYSIA

<sup>3</sup> HO CHI MINH CITY UNIVERSITY OF TECHNOLOGY (HCMUT), VNU-HCM KEY LABORATORY FOR MATERIALS TECHNOLOGY, 268 LY THUONG KIET STREET, DISTRICT 10, HO CHI MINH CITY, VIETNAM

<sup>4</sup> VIETNAM NATIONAL UNIVERSITY HO CHI MINH CITY, LINH TRUNG WARD, THU DUC CITY, HO CHI MINH CITY, VIETNAM

<sup>5</sup> UNIVERSITI SAINS MALAYSIA, ENERGY MATERIALS RESEARCH GROUP (EMRG), SCHOOL OF MATERIALS AND MINERAL RESOURCES ENGINEERING, 14300, NIBONG TEBAL, PULAU PINANG, MALAYSIA

<sup>6</sup> KING FAISAL UNIVERSITY, DEPARTMENT OF PHYSICS, COLLEGE OF SCIENCE, AL-HASSA, P.O. BOX 400, HOFUF, 31982, SAUDI ARABIA

through strong affinity with Sn. Previous studies reported that 5 wt.% Ni coating on micro-sized PCC fillers optimized performance by promoting interaction with the Sn matrix [15]. However, limited studies have investigated the effects of Ni-coated ceramic fillers of varying sizes, including micrometer- and nanometer-scale PCC, on the critical reliability aspects of composite solders, such as wettability, thermal stability, and hardness.

This study aims to evaluate the impact of adding Ni-coated micro- and nano-sized PCC fillers on the structural, thermal, and mechanical properties of eutectic Sn-9Zn composite solders. The findings are supported by microstructural, phase, and elemental analyses to provide insights into the role of Ni-coated fillers in improving the performance of Sn-Zn solders.

#### 2. Experimental materials and method

To synthesize Ni-coated PCC (Ni-PCC), hydrated nickel chloride (NiC<sub>12</sub>·6H<sub>2</sub>O), 20 g of micro- or nano-sized PCC, and sodium hypophosphite (NaH<sub>2</sub>PO<sub>2</sub>) were mixed in a 1:1:1 ratio in heated water (80°C) and stirred at 400 rpm (Fig. 1). The pH of the solution was adjusted to 8 by adding drops of sodium hydroxide while maintaining the temperature. Additional NaH<sub>2</sub>PO<sub>2</sub> was introduced at a 1:1 ratio with NiCl<sub>2</sub>·6H<sub>2</sub>O, maintaining a 5% concentration, to produce 5% Ni coating on PCC. After cooling, the resulting product was filtered, dried, and ground into fine powder using a mortar and pestle.

Composite solders were prepared by incorporating 0.5 wt.% PCC-based powders into the Sn-9Zn master alloy through casting process, at the processing temperature of 300°C. The mixtures were melted in an inert crucible at 550°C and allowed to cool

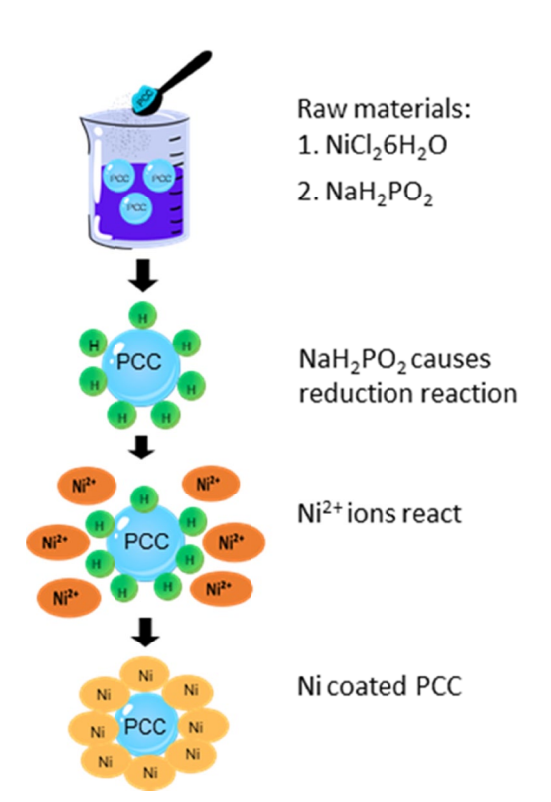


Fig. 1. Schematic diagram of Ni-coating process on PCC

to ambient temperature. Samples produced included Sn-9Zn (SZ), Sn-9Zn with 0.5 wt.% micro-PCC (SZMP), Sn-9Zn with 0.5 wt.% nano-PCC (SZNP), Sn-9Zn with 0.5 wt.% of 5% Nicoated micro-PCC (SZNMP), and Sn-9Zn with 0.5 wt.% of 5% Ni-coated nano-PCC (SZNNP). The solidified composite solders were rolled manually to a 0.5 mm thickness and then punched into 5 mm-diameter pellets. The prepared samples were characterized for phase composition using X-ray diffraction (XRD, Shimadzu XRD 6000) and thermal properties through differential scanning calorimetry (DSC, DSC-8000 Perkin Elmer). Microstructural and elemental analyses were performed using scanning electron microscopy (SEM, JEOL JSM-6460-LA equipped with energy dispersive spectroscopy (EDS)) and transmission electron microscopy (TEM, FEI Tecnai G2 20 S-Twin). Hardness testing was conducted with a Vickers microhardness tester (Sinowon) at a 0.1 kgf load and 10-second dwell time.

### 3. Results and discussion

# 3.1. Microstructure and zeta potential analyses of nickel-coated precipitated calcium carbonate

The uncoated micro-PCC exhibits a smooth surface with minimal agglomeration, as observed in the TEM analysis (Fig. 2a). In contrast, noticeable agglomerations are evident in the nano-PCC sample (Fig. 2b). Following the Ni coating of the micro-PCC, the surface appears darker with no significant agglomeration detected. However, the Ni coating has little effect in preventing agglomeration in the nano-PCC (Fig. 2c-d). Moreover, the Ni distribution on the nano-PCC is uneven, with several Ni agglomerates clearly visible.

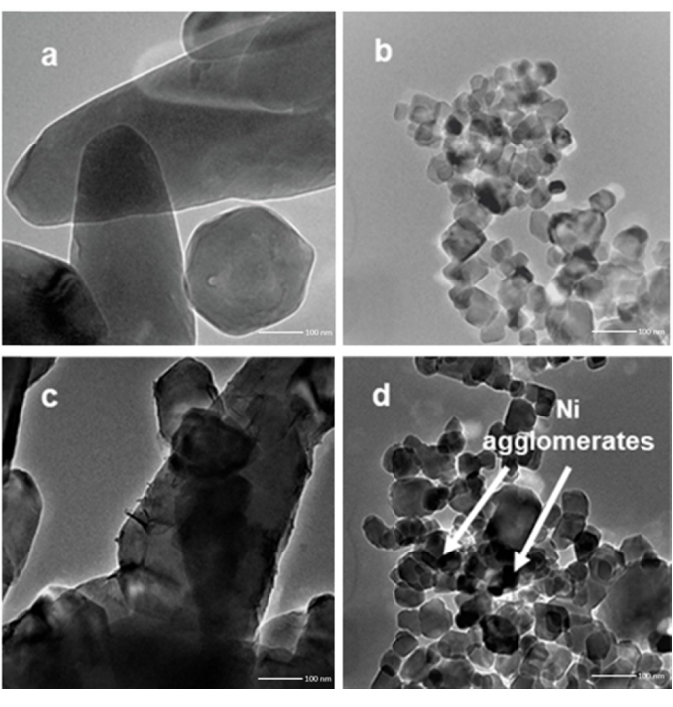


Fig. 2. TEM results for (a) micro-PCC, (b) nano-PCC, (c) Ni-coated micro-PCC, and (d) Ni-coated nano-PCC

To evaluate the impact of Ni coating on PCC dispersion in ceramic-reinforced composite solder, Zeta potential measurement was conducted (Fig. 3). The micro-PCC particles exhibited a Zeta potential of -3.39 mV, indicating a net negative surface charge with relatively weak repulsive forces between particles. In contrast, the Ni-coated micro-PCC particles showed a Zeta potential of -11.9 mV, suggesting a stronger repulsive force and successful particle separation due to the surface coating [16]. For the nanoparticles, the Zeta potential shifted from -12.8 mV to -9.92 mV after Ni coating. This indicates that the Ni coating failed to effectively de-agglomerate the nano-PCC. Nanoparticles typically exhibit higher Zeta potential values due to their increased surface reactivity, which enhances surface charge generation or ionization and reinforces electrostatic attraction between particles [17]. Moreover, nanoparticles possess a high surface-to-volume ratio, resulting in a larger proportion of atoms or molecules on the surface compared to the bulk. As a result, surface properties become more dominant, promoting agglomeration [18]. This explains the inability of Ni coating to effectively separate nano-PCC particles.

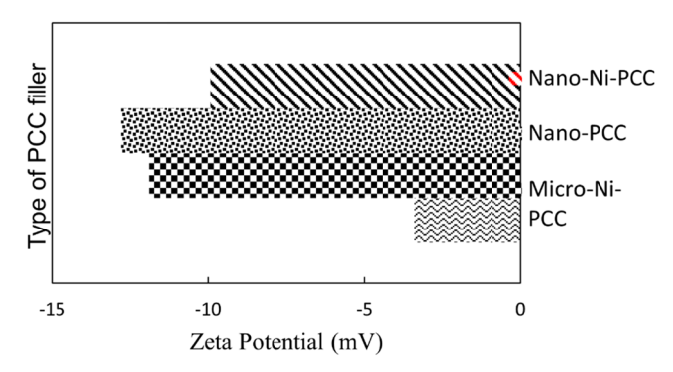


Fig. 3. The effect of Ni coating on Zeta potential of PCC

Particles with a neutral charge tend to aggregate naturally, often forming larger clusters due to gravitational or van der Waals forces [10] (Fig. 4a). Electroless Ni plating, which involves depositing a uniform metal layer onto particle surfaces through a controlled chemical reduction process without the need for external electricity, addresses this issue. This method not only produces a smooth and cohesive metal coating but can also modify or enhance surface charges on the particles [19]. The newly applied metallic layer may generate a surface potential that induces repulsive electrostatic forces between particles (Fig. 4b). As the particles acquire similar charges during the plating process, they experience mutual repulsion, effectively reducing the likelihood of aggregation.

### 3.2. Phase analysis of composite solders

As shown in Fig. 5a, the XRD pattern of the raw PCC revealed distinct peaks at  $24.0^{\circ}$  (012),  $29.0^{\circ}$  (104),  $35.0^{\circ}$  (006),  $47.5^{\circ}$  (110),  $56.6^{\circ}$  (113),  $62.4^{\circ}$  (202),  $62.8^{\circ}$  (018), and  $65.0^{\circ}$  (125). These peaks correspond to calcium carbonate (ICDD

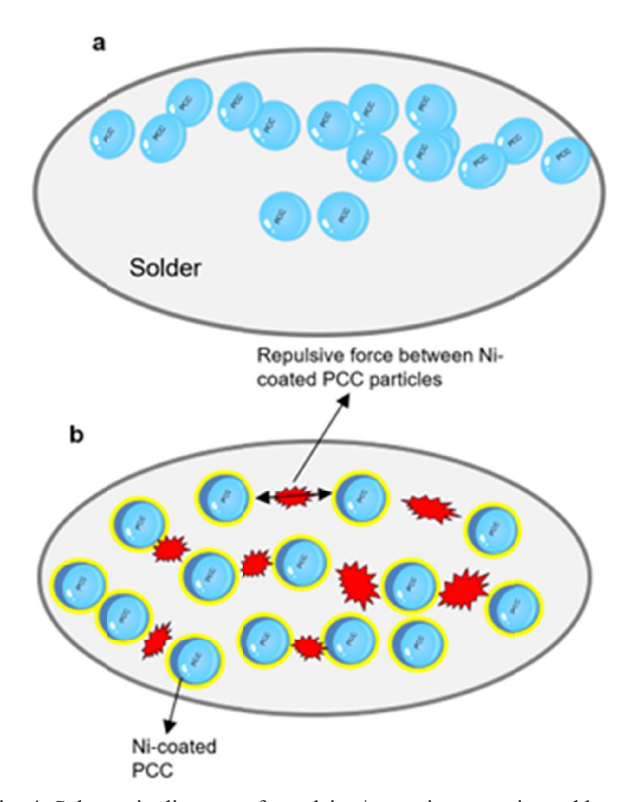
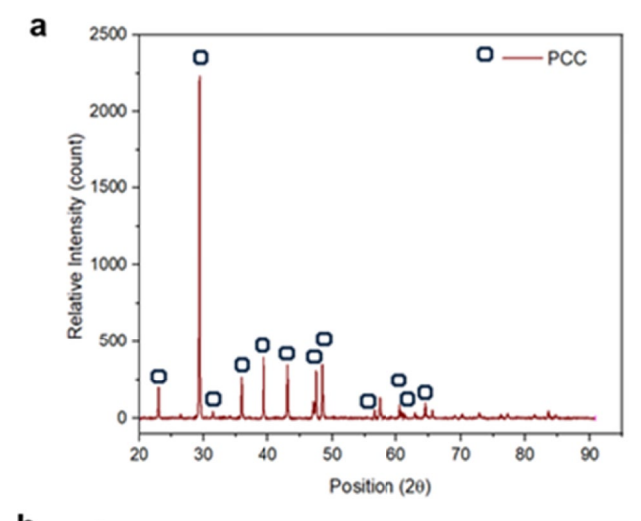


Fig. 4. Schematic diagram of repulsion/attraction experienced by zeta potential of (a) unmodified and (b) Ni-coated PCC



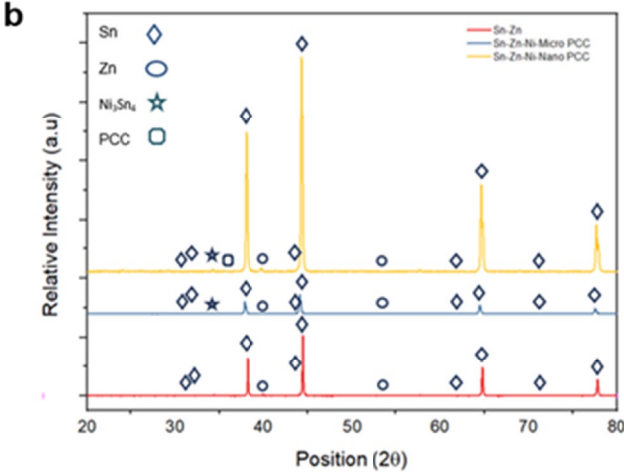


Fig. 5. XRD spectra of (a) PCC and (b) Ni-PCC composite solders

01-072-1937) and align well with previously reported data [9]. For the Sn-9Zn solder, peaks associated with Sn (ICDD 00-001-0926) and Zn (ICDD 00-001-1238) were identified (Fig. 5b). The Sn peaks appeared at 31.05° (200), 31.30° (101), 44.29° (220), 44.42° (211), 63.08° (400), 65.11° (321), 72.75° (420), and 79.82° (312). Meanwhile, Zn peaks were observed at 43.79° (101) and 54.82° (102). The absence of any new intermetallic phases in this alloy can be attributed to the limited solubility of the constituent elements, which restricted their mutual interaction [20].

For the Sn-9Zn alloy containing 5% Ni-PCC in both micro- and nano-forms, additional peaks corresponding to Ni<sub>3</sub>Sn<sub>4</sub> (ICDD 03-065-4310) and PCC were observed. The appearance of the Ni<sub>3</sub>Sn<sub>4</sub> phase confirms the successful interaction between Ni and Sn [9]. This intermetallic compound (IMC) formed through diffusion between the Ni coating layer and Sn during the melting process, serving as a "bridging material" between the reinforcements and the solder matrix.

The Ni coating process begins with the precursor, Na<sub>2</sub>H<sub>2</sub>PO<sub>4</sub>, undergoing a reduction reaction that releases a hydrogen atom, which subsequently binds to the PCC surface (Eq. (1)). Following this, Ni<sup>2+</sup> ions from NiCl<sub>2</sub>· 6H<sub>2</sub>O and H<sub>2</sub>PO<sub>2</sub><sup>-</sup> ions are reduced, leading to the deposition of nickel atoms (Eqs. (2)-(4)). Experimental results demonstrated that the interaction between H<sub>2</sub>PO<sub>2</sub><sup>-</sup> and water facilitated the deposition of Ni atoms onto the PCC surface, where they bonded securely, through the reaction [21]:

$$(H_2PO_2)^- + H_2O \rightarrow H^+ + (H_2PO_2)^{2-} + 2H$$
 (1)

$$Ni^{2+} H_2PO_2^- + H_2O \rightarrow Ni + H_2PO_3^- + 2H$$
 (2)

$$H_2PO_2^- + H_2O \rightarrow H_2PO_3^- + H_2$$
 (3)

$$Ni^{2+} + 2H_2PO_2^- \rightarrow Ni + 2H_2PO_3^- + 2H^+ + H_2$$
 (4)

The incorporation of the Ni<sub>3</sub>Sn<sub>4</sub> compound within a tin solder matrix offers several advantageous properties for solder joints. Research on Ni-coated SiC particles in a SAC solder matrix has demonstrated that Ni-coated SiC improves the wetting angle of composite solder [12]. Similarly, prior studies [22] have shown that embedding Ni-coated graphene (Ni-GNS) in the SAC305 solder matrix enhances both the mechanical strength and hardness of the solder joint. These enhancements contribute to improving the overall durability and reliability of the solder joint.

# 3.3. Microstructure and elemental analyses of composite solders

The eutectic SZ solder exhibits a distribution of Zn-rich phases appearing as black, needle-like structures randomly dispersed within the light-contrast  $\beta$ -Sn matrix (Fig. 6a). These black structures form due to the limited mutual solubility of the elements, as previously reported [23]. For SZ solder, the

average size of the Zn-rich phase is  $431.8 \pm 25.4$  µm. In contrast, the SZNMP shows a reduction in Zn-rich phase size to  $203.2 \pm 15.24$  µm (Fig. 6b).

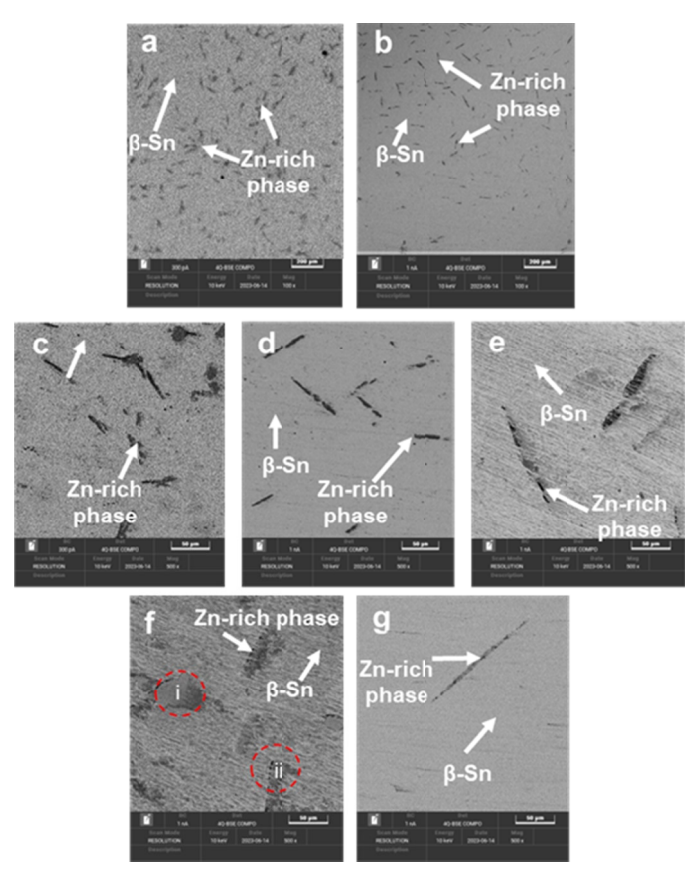


Fig. 6. SEM results for  $100\times$  magnification of (a) SZ, (b) SZMP, and  $500\times$  magnification (c) SZ, (d) SZNMP, (e) SZNNP, (f) SZNP and (g) SZMP

At higher magnification, small Zn-rich phases are visible in both SZ (Fig. 6c) and SZNMP (Fig. 6d). However, significant increases in Zn-rich phase size are observed for SZNNP (Fig. 6e), SZMP (Fig. 6g), and SZNP (Fig. 6f). The average Zn-rich phase sizes recorded were 279.4  $\pm$  15.24  $\mu m$  (SZNNP), 482.6  $\pm$  15.24  $\mu m$  (SZMP), and 508  $\pm$  81.28  $\mu m$  (SZNP). Notably, agglomerated fillers were observed on the surface of SZNP (Fig. 6f, marked in red). According to EDS analysis, spot i contains Ca (2.1 wt.%), C (1.89 wt.%), O (3.27 wt.%), Sn (47.74 wt.%), and Zn (45 wt.%), while spot ii contains Ca (0.86 wt.%), C (15.11 wt.%), O (15.19 wt.%), Sn (8.59 wt.%), and Zn (60.24 wt.%). The presence of Ca, C, and O on the solder surface suggests the possibility of filler expulsion occurring in SZNP.

The reduction in Zn-rich phase size is attributed to enhanced grain nucleation through heterogeneous nucleation during solidification. The ceramic filler particles act as nucleation sites, facilitating grain growth during solidification, as recently discussed [24]. The smallest Zn-rich phase size observed in SZNMP indicates that 5 wt.% Ni coating on micro-PCC provides the most uniform distribution with minimal agglomeration. In contrast, the increased Zn-rich phase sizes in SZNNP, SZMP, and SZNP

may result from less effective PCC distribution and the presence of agglomerates, as seen in Fig. 6f.

The corresponding EDS analysis reveals that the pristine SZ solder consists of Sn (90.49 wt.%) and Zn (9.51 wt.%) (Fig. 7a). This composition aligns with the raw materials used and confirms proper fabrication. Incorporating 0.5 wt.% micro-PCC into SZ introduces 3.50 wt.% Ca, 0.02 wt.% C, and 0.19 wt.% O (Fig. 7b), with the remaining composition comprising Sn (87.19 wt.%) and Zn (9.10 wt.%). Notably, the addition of nano-PCC significantly elevates the Zn content to 60.24 wt.% (Fig. 7c), which correlates closely with the enlarged Zn-rich phase observed earlier. When Ni coating is introduced, the presence of Ni is confirmed in the energy spectra for both micro- (Fig. 7d) and nano-PCC (Fig. 7e) composite solders. Furthermore, Zn content is notably lower in SZMNP (5.82 wt.%) compared to 19.96 wt.% in SZNNP. This finding corresponds with the smaller Zn-rich phase detected in SZMNP.

### 3.5. Hardness analysis of composite solders

The Vickers microhardness measurements were taken at five different points to calculate the average value (Fig. 8a). The pristine SZ exhibited a hardness of  $15.14 \pm 1.06$  HV, which significantly increased to  $16.98 \pm 0.89$  HV for SZNMP (Fig. 8b). Following this, SZNP showed a hardness of  $16.16 \pm 0.63$  HV, while SZNNP recorded  $14.78 \pm 1.31$  HV. The lowest hardness was observed for SZMP. The addition of Ni-PCC notably improved the hardness, with the most pronounced effect seen in SZNMP. The nickel coating on PCC particles reinforces the solder matrix, enhancing its strength by contributing to the hardness and mechanical properties of the solder. This reinforcement provides additional support and increases resistance to deformation. Furthermore, the Ni coating facilitates better reinforcement distribution (Fig. 8c), effectively limiting the diffusion of elements in the lead-free solder during the reflow

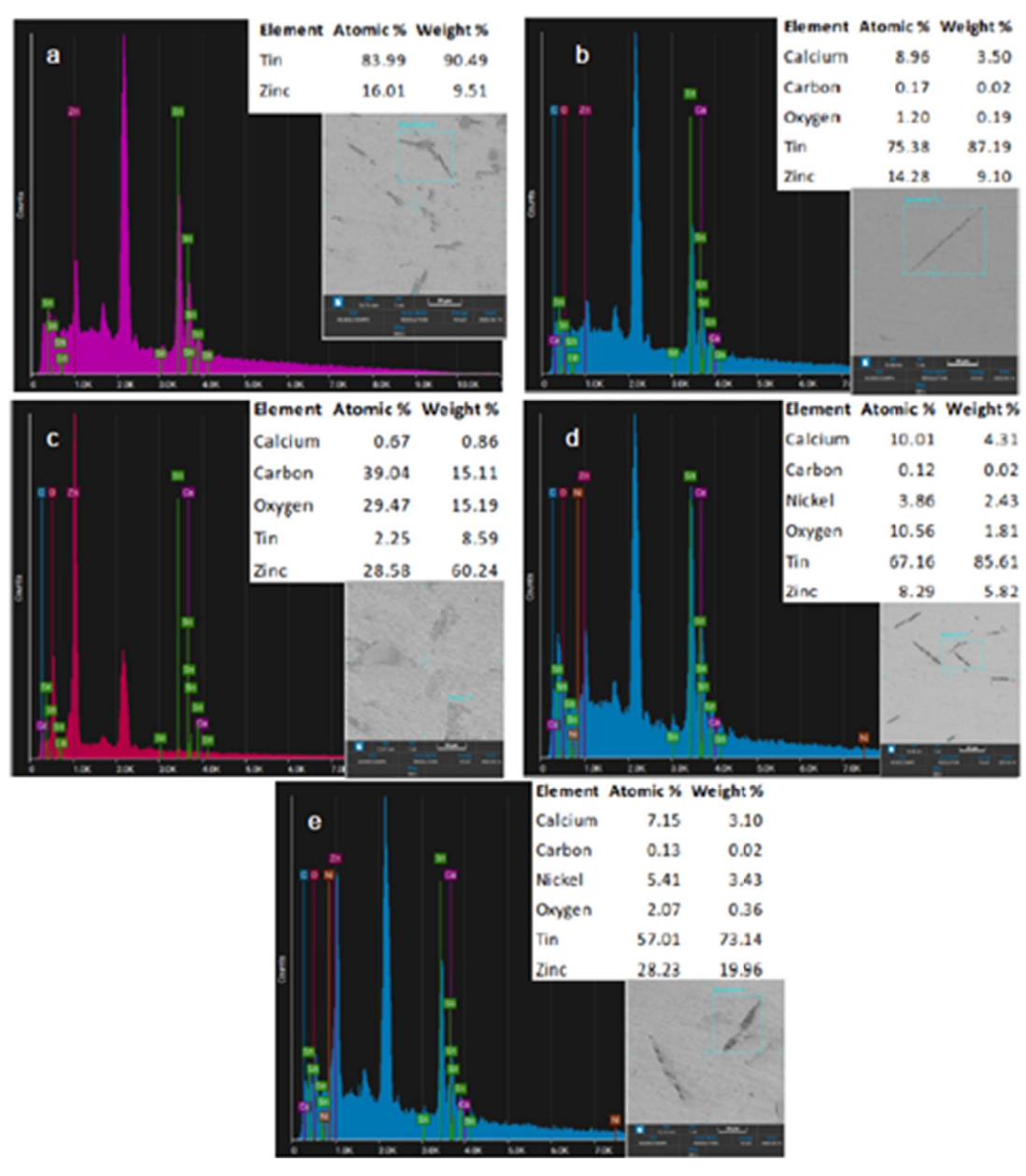


Fig. 7. EDS analysis pertaining to the solder area (a) SZ, (b) SZMP, (c) SZNP, (d) SZNMP and (e) SZNNP

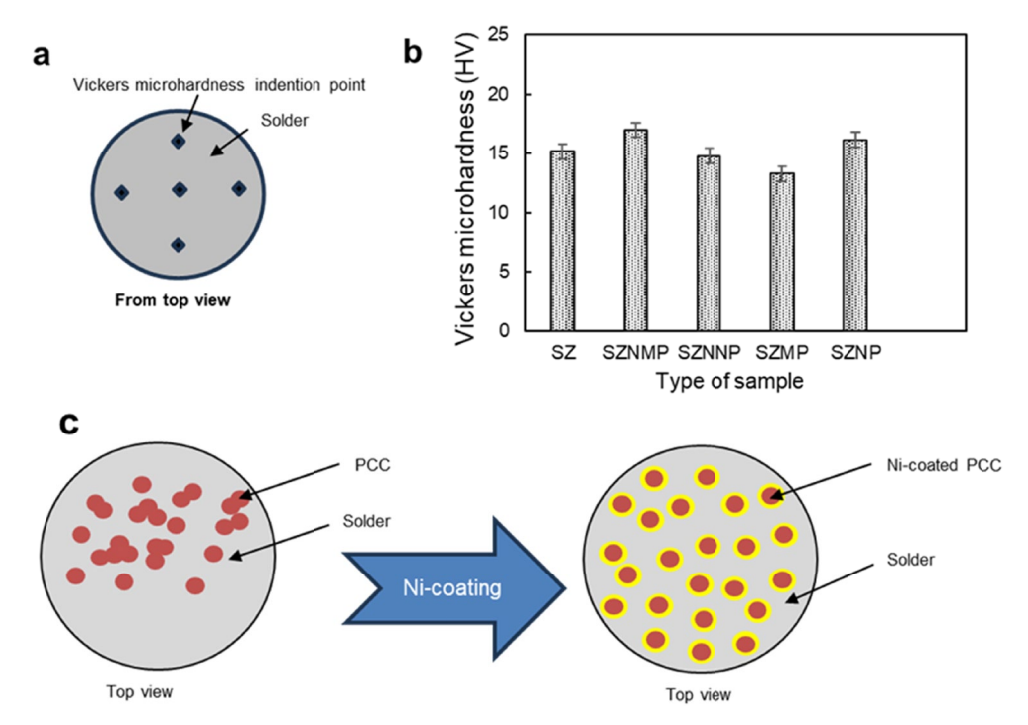


Fig. 8. (a) Schematic drawings of Vickers microhardness indention points, (b) average Vickers microhardness value of composite solder and (c) schematics on better distribution of PCC due to the Ni coating

process. The presence of a smaller Zn-rich phase, as observed in the microstructural analysis, inhibits the slip mechanism during hardness testing and strengthens the solder via the Zener pinning effect [25].

## 4. Conclusion

The study examined the impact of Ni coating on micro- and nano-sized PCC particles and its influence on the microstructure, phase composition, and hardness of Sn-9Zn composite solder. The findings are as follows:

- i. The Ni coating effectively reduces the agglomeration of PCC fillers, particularly in micro-PCC. When Ni-coated PCC is incorporated into the SZ solder, the formation of  $\mathrm{Ni}_3\mathrm{Sn}_4$  indicates a successful interaction between Ni and Sn
- ii. Adding Ni-coated PCC improves the hardness of Sn-Zn solder, with SZNMP solder exhibiting the highest micro-Vickers hardness among the tested compositions. This improvement is attributed to the enhanced distribution of PCC particles.

In summary, incorporating nickel-coated micro-PCC particles into Sn-Zn solder composites significantly improves their performance across various metrics, making them more suitable for soldering applications. For future works, long-term reliability testing including conducting thermal cycling and mechanical fatigue tests to assess the durability and performance of Nicoated PCC-reinforced solder under real-world conditions, and investigation on the wettability and interfacial behavior between the solder and substrate materials.

#### Acknowledgments

This research was funded by by the Fundamental Research Grant Scheme (FRGS) FRGS/1/2019/TK05/UNIMAP/02/5 and FRGS/1/2024/TK09/USM/02/7), Ministry of Higher Education, Malaysia. This work was supported by the Deanship of Scientific Research, Vice Presidency for Graduate Studies and Scientific Research, King Faisal University, Saudi Arabia [Grant No. KFU250451].

### REFERENCES

- T. Gancarz, J. Pstruś, Characteristics Of Sn-Zn Cast Alloys With The Addition Of Ag And Cu, Archives of Metallurgy and Materials 60(3), 1603-1607 (2015).
- [2] D.-H. Jung, J.-P. Jung, Review of the wettability of solder with a wetting balance test for recent advanced microelectronic packaging. Critical Reviews in Solid State and Materials Sciences 44 (4), 324-343 (2019).
- [3] B. Wang, Y. Wu, W. Wu, H. Wang, K. Zhang, Fabrication and properties of NiO-modified Al2O3 reinforced Sn1. 0Ag0. 5Cu composite solder and soldering performance. Journal of Materials Science 57 (36), 17491-17502 (2022).
- [4] A. Skwarek, O. Krammer, T. Hurtony, P. Ptak, K. Górecki, S. Wroński, D. Straubinger, K. Witek, B. Illés, Application of ZnO nanoparticles in Sn99Ag0. 3Cu0. 7-based composite solder alloys. Nanomaterials 11 (6), 1545 (2021).
- [5] N.S.M. Zaimi, M.A.A.M. Salleh, A.V. Sandu, M.M.A.B. Abdullah, N. Saud, S.Z.A. Rahim, P. Vizureanu, R.M. Said, M.I.I. Ramli, Performance of Sn-3.0 Ag-0.5 Cu Composite Solder with Kaolin Geopolymer Ceramic Reinforcement on Microstructure

- and Mechanical Properties under Isothermal Ageing. Materials **14** (4), 776 (2021).
- [6] B. Illés, H. Choi, K. Szostak, J. Byun, A. Skwarek, Effects of CuO nanoparticles on SAC composite solder joints: Microstructural and DFT study. Journal of Materials Research and Technology 32, 609-620 (2024).
- [7] A. Skwarek, H. Choi, T. Hurtony, J. Byun, A.A. Mohamad, D. Bušek, K. Dušek, B. Illés, Effects of ZrO2 Nano-Particles' Incorporation into SnAgCu Solder Alloys: An Experimental and Theoretical Study. Nanomaterials 14 (20), 1636 (2024).
- [8] A. Skwarek, B. Illés, P. Górecki, A. Pietruszka, J. Tarasiuk, T. Hurtony, Influence of SiC reinforcement on microstructural and thermal properties of SAC0307 solder joints. Journal of Materials Research and Technology 22, 403-412 (2023).
- [9] W.K. Leong, A.A. Mohamad, M.F.M. Nazeri, Effect of the nickel coated precipitated calcium carbonate addition on microstructure, phase and wettability of Sn-9Zn solder. Journal of Physics: Conference Series, IOP Publishing, 2022, p. 012031.
- [10] W.K. Leong, A.A. Mohamad, M.F.M. Nazeri, Surface Modifications on Ceramic Reinforcement for Tin-Based Composite Solders, Recent Progress in Lead-Free Solder Technology: Materials Development, Processing and Performances, Springer 2022, pp. 53-75.
- [11] L. Duo, C. Bin, J. Guobiao, S. Yanyu, Q. Zhang, S. Xiaoguo, C. Jian, Interfacial characteristics in CNTs-AgCuTi systems. Chinese Journal of Aeronautics 35 (4), 450-460 (2022).
- [12] M.K. Pal, G. Gergely, D. Koncz-Horváth, Z. Gácsi, Characterization of the interface between ceramics reinforcement and lead-free solder matrix. Surfaces and Interfaces 20, 100576 (2020).
- [13] S. Wang, Q. Zhao, P. Xing, Y. Zhuang, L. Wang, Influence of dispersant on the microstructure and performance of the hot-pressed B4C-YB4 ceramics. Journal of the Australian Ceramic Society 1-13 (2023).
- [14] V. Morales-Florez, A. Dominguez-Rodriguez, Mechanical properties of ceramics reinforced with allotropic forms of carbon. Progress in Materials Science 128, 100966 (2022).
- [15] K. Leong, F. Zainal, M. Kasmuin, A. Mohamad, M. Nazari, M. Nabiałek, B. Jeż, Wettability and Hardness Investigation of Nickel-Coated Precipitated Calcium Carbonate Sn-9Zn Composite Solder. Archives of Metallurgy and Materials 1035-1040 (2023).

- [16] B. Gaba, T. Khan, M.F. Haider, T. Alam, S. Baboota, S. Parvez, J. Ali, Vitamin E loaded naringenin nanoemulsion via intranasal delivery for the management of oxidative stress in a 6-OHDA Parkinson's disease model. J. Bio. Med. Research International 2019 (2019).
- [17] M.S. Kuyukina, M.V. Makarova, O.N. Pistsova, G.G. Glebov, M.A. Osipenko, I.B. Ivshina, Exposure to metal nanoparticles changes zeta potentials of Rhodococcus cells. Heliyon 8 (11) (2022).
- [18] H.-K. Lee, H.-Y. Lee, J.-M. Jeon, Codeposition of micro-and nano-sized SiC particles in the nickel matrix composite coatings obtained by electroplating. Surface and Coatings Technology 201 (8), 4711-4717 (2007).
- [19] A. Chakraborty, N.M. Nair, A. Adekar, P. Swaminathan, Templated electroless nickel deposition for patterning applications. Surface and Coatings Technology 370, 106-112 (2019).
- [20] M.F.M. Nazeri, A.A. Mohamad, Polarization study of Sn-9Zn lead-free solder in KOH solutions. Int. J. Electroactive Mater. 2, 34-39 (2014).
- [21] P. Zhang, Z. Lv, X. Liu, G. Xie, B. Zhang, Electroless nickel plating on alumina ceramic activated by metallic nickel as electrocatalyst for oxygen evolution reaction. Catalysis Communications 149, 106238 (2021).
- [22] G. Chen, F. Wu, C. Liu, V.V. Silberschmidt, Y. Chan, Microstructures and properties of new Sn–Ag–Cu lead-free solder reinforced with Ni-coated graphene nanosheets. Journal of Alloys and Compounds 656, 500-509 (2016).
- [23] M. Islam, Y. Chan, M. Rizvi, W. Jillek, Investigations of interfacial reactions of Sn–Zn based and Sn–Ag–Cu lead-free solder alloys as replacement for Sn–Pb solder. Journal of Alloys Compounds 400 (1-2), 136-144 (2005).
- [24] L. Xingyi, L. Ling, S. Yanyu, L. Duo, H. Shengpeng, S. Xiaoguo, C. Jian, Wetting behavior of AgCu-4.5 Ti filler reinforced by carbon nanotubes on C/C composite. Chinese Journal of Aeronautics 34 (12), 205-213 (2021).
- [25] L. Zhang, K.N. Tu, Structure and properties of lead-free solders bearing micro and nano particles. Materials Science and Engineering: R: Reports 82, 1-32 (2014).